Photoinduced Catalysis of Redox Reactions. Turnover Numbers, Turnover Frequency, and Limiting Processes: Kinetic Analysis and Application to Light-Driven Hydrogen Production

Cyrille Costentin, Fakourou Camara, Jérôme Fortage, Marie-Noëlle Collomb

Photoinduced Catalysis of Redox Reactions. Turnover Numbers, Turnover Frequency and Limiting Processes: Kinetic Analysis and Application to Light-Driven Hydrogen Production.

Cyrille Costentin,*[a,b] Fakourou Camara,[a] Jérôme Fortage,[a] and Marie-Noëlle Collomb[a]

[a] Univ Grenoble Alpes, DCM, CNRS, 38000 Grenoble, France. [b] Université Paris Cité, 75013 Paris, France.

ABSTRACT: The energy of light is likely to be used to drive thermodynamically unfavorable redox reactions with the goal of storing energy in chemical bonds, for example via hydrogen production. To that end molecular systems involving at least four components (substrate, photosensitizer, sacrificial donor and catalyst) are designed as a step toward building photoelectrochemical devices. The efficiency of such photoinduced catalysis of redox reactions is often reported as turnover numbers over time, leading to maximal turnover numbers and initial turnover frequencies. How these figures of merit are related to the properties of the system (light absorption, excited state quenching, catalytic rate constants, back electron transfers etc...) is however lacking, thus making reliable comparison of systems difficult. Herein we propose a general analytical kinetic framework for the analysis of photoinduced catalytic processes. In particular we show that, even for ideal systems, the turnover number does not increase linearly with time due to increasing unproductive cycles over time via back electron transfers. We then incorporate limiting processes corresponding to photosensitizer or catalyst degradation in the kinetic analysis and we provide analytical expressions for the maximal turnover numbers in such situations. Finally, the kinetic model is used to successfully rationalize experimental data corresponding to light-driven hydrogen production in water using ascorbate as sacrificial donor, a cobalt tetrazamacrocyclic complex as catalyst and two different photosensitizers, the classical $[Ru(bpy)_3]^{2+}$ and a robust triazatriangulenium organic dye $TATA^+$.

Introduction

Using the energy of light to drive thermodynamically unfavorable redox reactions is at the core of contemporary energy challenges. [1-7] For instance, photoinduced catalytic systems for water oxidation into O_2,[8-14] proton (water) reduction into H_2 [15-21] [22-28] and CO_2 reduction [29-33] have been extensively developed in homogeneous solution during the last two decades as a first step toward building photoelectrochemical devices. These systems can be purely molecular or hybrid, combining molecular and inorganic components. A typical homogeneous molecular system involves a minimal number of four components a photosensitizer (PS), a catalyst (Cat_{ox}), a sacrificial electron donor (SD) or acceptor (SA) and the substrate (S_{ox}), that can be the solvent. In such systems, the photo-induced electron transfer processes leading to the catalytic reaction are initiated by the absorption of light by the PS leading to its conversion to an excited state (PS*). It is exemplified in Scheme 1 in the case of a model light-driven one electron reduction (S_{ox} + SD -> P_{red} + $SD^{\bullet+}$). Because the excited state of the photosensitizer PS* is usually both a strong reductant and a strong oxidant, two pathways are in competition, namely a reductive quenching mechanism and an oxidative quenching mechanism (Scheme 1).[34,35] [36,37] In the case of reductive quenching (Scheme 1a), PS* is efficiently quenched by the sacrificial donor (SD)[38] to form an homogeneous reductant ($PS^{\bullet-}$) which then reduces the molecular catalyst (Cat_{ox}) to its active form, Cat_{red}, while reforming the ground-state PS. Cat_{red} then acts as the actual homogeneous reductant of the substrate (S_{ox}). Note that two back electron transfers from either $PS^{\bullet-}$ or Cat_{red} to $SD^{\bullet+}$ can render the absorption of light unproductive regarding the redox reaction. [39] Alternatively, in the oxidative quenching pathway (Scheme 1b), PS* is efficiently quenched by the catalyst itself (Cat_{ox}) to form its active form, Cat_{red}, while generating $PS^{\bullet+}$. Cat_{red} then acts as the actual homogeneous reductant of the substrate (S_{ox}) whereas the ground state photosensitizer is regenerated via electron transfer to the sacrificial donor SD. Again two back electron transfers from Cat_{red} to either $SD^{\bullet+}$ or $PS^{\bullet+}$ can render the absorption of light unproductive regarding the redox reaction. For a given targeted conversion of S_{ox} to P_{red}, the large number and diversity of available combination of SD, PS, and Cat_{ox} requires the development of tools for comparing one to another. Besides mandatory thermodynamic considerations that have been used as guidelines in the choice of the various components, it seems timely to focus on kinetic criteria.

So far, the efficiency of photoinduced catalytic systems is mainly reported as turnover frequencies or turnover numbers as well as sometimes quantum yields. How these first two figures of merit relate to the various steps of the mechanisms depicted in Scheme 1 and their corresponding rate constants remains however largely elusive. In the present contribution, we provide a first approach to this issue by developing a formal kinetic framework for photoinduced catalytic processes. As these processes are diverse and complex, it is not possible to propose a kinetic

model covering all experimental situations. Considering that in many experimental systems the sacrificial donor is in large excess over the catalyst, we will only consider a reductive quenching process. To reach a degree of generality, we will also only consider the minimal set of chemical steps. In that regards, the reaction scheme depicted in Scheme 1a (and the corresponding rate constants defined in the scheme) captures ideal systems with no degradation of any of the components (PS or Cat). This system is analyzed in a first place with particular emphasis on the effect of back electron transfer steps. In order to get a realistic kinetic model, the additional effect of various degradation pathways is then analyzed and discussed. Finally, the kinetic model is used to rationalize previously reported experimental data on light-driven hydrogen production in water. This will require adaptation of the kinetic model to two electrons reduction processes.

Scheme 1. Photo-induced catalysis of redox reactions

(a) Reductive quenching

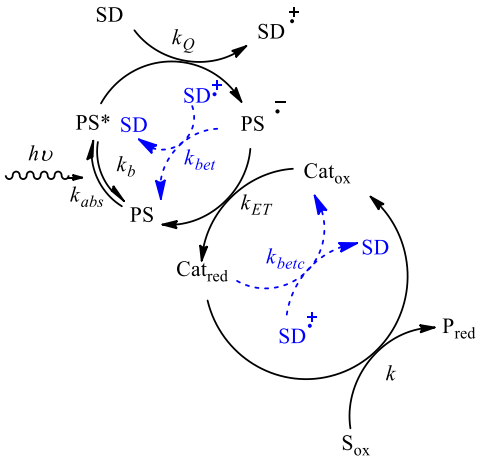

(b) Oxidative quenching

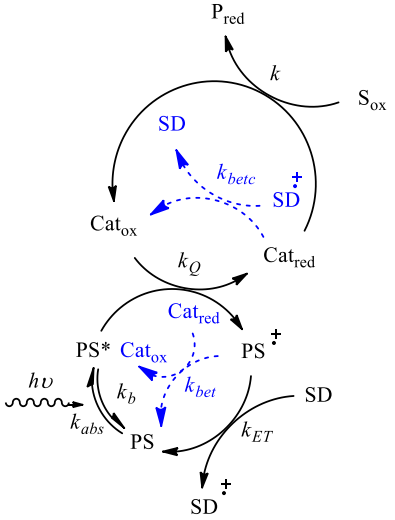

Results and Discussion

We consider a redox reaction S_{ox} + SD -> P_{red} + $SD^{\bullet+}$ where S_{ox} is the targeted substrate and SD a sacrificial electron donor. The reaction is uphill and requires the energy of light to be driven. Although reactions of interest are usually more complex often involving multiple electron transfers, the minimal set of steps depicted in Scheme 1 provides the essential features of the problem in ideal conditions, i.e. no degradation of any component. As additional general simplifications, we consider that the SD is in excess so that its concentration is considered as constant during the reaction and the reductive pathway (Scheme 1a) is the only pathway. We also assume that the process is irreversible in the sense that the final products, P_{red} and $SD^{\bullet+}$, do not react with each other to give back the reactants although this process is thermodynamically favorable. As already indicated, irreversible sacrificial electron donors are used to decrease back electron transfers. However, in some cases, the final oxidized form of the sacrificial donor accumulating in solution can undergo back electron transfers. Therefore, for the sake of simplicity, we consider a simple $SD^{\bullet+}$/SD couple capturing the essential features of a typical sacrificial donor. Finally, all intermediates are assumed to be at steady-state and hence do not accumulate.

In all cases considered in the following, the observable is the concentration of the product P_{red} formed over time. Depending on the operating conditions, the evolution of the reaction can be reported with different metrics. If the substrate is consumed during the experiment, it is convenient to introduce the yield of conversion. Alternatively, if experiments are performed with large excess of substrate (typically when the solvent is the substrate), the useful metrics is the turnover number (*TON*). In the following, we will only consider the situation where the substrate is in large excess. Definition of the *TON* requires attention as two different definitions can be introduced. The number of product made relative to the number of catalyst, TON_{cat} :

$$TON_{cat} = \frac{[\mathrm{P_{red}}]_t}{[\mathrm{Cat_{ox}}]_0} \qquad (1)$$

or the number of product made relative to the number of photosensitizer, corresponding to the photocatalytic turnover number,

$$TON_{PS} = \frac{[\mathrm{P_{red}}]_t}{[\mathrm{PS}]_0} \qquad (2)$$

where $[\mathrm{Cat_{ox}}]_0$ and $[\mathrm{PS}]_0$ are the introduced concentrations of Cat_{ox} and PS. In modeling photoinduced catalysis of redox reactions, we will focus on TON_{cat} as it is the quantity usually reported in the literature. Finally, the corresponding turnover frequency (*TOF*) can be defined for each of these quantities as the time derivative:

$$TOF = \frac{d(TON)}{dt} \qquad (3)$$

However, as shown below, except for specific conditions, the time evolution of the product concentration is not linear and therefore the TOF is not a constant; the reported value is then its initial value TOF_0.

Photoinduced catalytic mechanisms are initiated by light absorption by PS to form the excited state PS*. We describe this process kinetically as a first-order reaction characterized by a rate constant k_{abs} (s^{-1}) which depends on the light source power but also on experimental conditions such as the reactor geometry and all the parameters that determine how much light is ultimately absorbed by the photocatalytic solution. The excited state has a lifetime characterized by the corresponding first order rate constant k_b (s^{-1}). Throughout our analysis, we make the assumption that $k_{abs} << k_b$ corresponding to situations where, under illumination, the resting state of the photosensitizer is PS. In the presence of a sacrificial donor SD, the excited state is reductively quenched with an efficiency characterized by the dimensionless parameter $p_Q = \frac{k_Q[\mathrm{SD}]}{k_b + k_Q[\mathrm{SD}]}$ (k_Q is the quenching rate constant in $M^{-1}s^{-1}$). The formation of the reduced photosensitizer $PS^{\bullet -}$ triggers a photoinduced catalysis that we now analyze.

Photoinduced catalysis: ideal system

Although the reduced photosensitizer $PS^{\bullet -}$ may be a good reductant in terms of outersphere electron transfer, it may not be able to interact efficiently with the substrate S_{ox}. The ideal scheme is thus the one depicted in Scheme 1a and the process referred to as a "photoinduced-catalysis of the redox reaction". In such a framework, it is shown in the Supporting Information (SI) that the time evolution of the turnover number relative to the catalyst is given by a third order polynomial relationship:

$$TON_{cat} + \left(p_{bet} + \frac{p_{betc}}{\gamma} \right) \frac{(TON_{cat})^2}{2} + p_{bet} \frac{p_{betc}}{\gamma} \frac{(TON_{cat})^3}{3} = TOF_{cat,0} \times t \qquad (4)$$

with $TOF_{cat,0} = \gamma p_Q k_{abs}$, $\gamma = \frac{[\mathrm{PS}]_0}{[\mathrm{Cat_{ox}}]_0}$, $p_{bet} = \frac{k_{bet}}{k_{ET}}$, $p_{betc} = \frac{k_{betc}[\mathrm{PS}]_0}{k[\mathrm{S_{ox}}]_0}$ and $p_Q = \frac{k_Q[\mathrm{SD}]}{k_b + k_Q[\mathrm{SD}]}$. k_{ET} ($M^{-1}s^{-1}$) is the electron transfer rate constant, k_{bet} and k_{betc} ($M^{-1}s^{-1}$) the back electron transfer rate constants, k ($M^{-1}s^{-1}$) is the catalytic rate constant (Scheme 1). The system is ideal (no degradation pathway) and the substrate is in excess (its concentration maintained constant) hence, according to equation (4) $TON_{cat} \to \infty$ when $t \to \infty$. However, because of both back electron transfers and the gradual increase of $SD^{\bullet +}$ concentration, the pace of increase of TON_{cat}, i.e. the turnover frequency, is gradually decreasing, starting with the initial value $TOF_{cat,0} = \frac{k_Q[\mathrm{SD}]}{k_b + k_Q[\mathrm{SD}]} \frac{[\mathrm{PS}]_0}{[\mathrm{Cat_{ox}}]_0} k_{abs}$. This initial turnover frequency is independent on the catalytic rate constant k. As just mentioned, the deviation from linearity of TON_{cat} with time arises from back electron transfers either from the reduced photosensitizer or from the reduced catalysts. However, the first one, an outersphere electron transfer from the reduced form of the sensitizer to the oxidized sacrificial donor, is in competition with an outersphere electron transfer from the reduced sensitizer to the catalyst. Both electron transfers have large driving forces and therefore, in many cases, the competition parameter $p_{bet} = \frac{k_{bet}}{k_{ET}}$ is expected to be close to unity because both k_{bet} and k_{ET} are close to diffusion limit, unless the corresponding electron transfers stand in the Marcus inverted region. It thus expected from equation (4), that, in many cases, as soon as TON_{cat} is larger than few units, the second and third order terms are dominant over the first order term. This leads to a non-linear time evolution of TON_{cat} and also this makes the notion of $TOF_{cat,0}$ not useful. It is exemplified in Figure 1 where simulations of the evolution of TON_{cat} according to equation (4) are shown as function of the dimensionless parameter $TOF_{cat,0} \times t$.

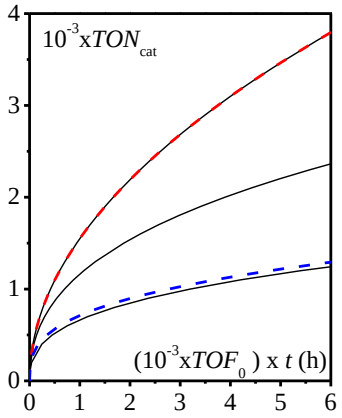

Figure 1. Time evolution of the turnover number in photoinduced catalysis of a redox reaction for an ideal system for various values of $\frac{p_{betc}}{\gamma} = 0, 10^{-3}, 10^{-2}$ (from top to bottom) and $p_{bet} = 3$ (black lines). The dashed red line corresponds to the second order term alone when $\frac{p_{betc}}{\gamma} = 0$: $TON_{cat} = \sqrt{2TOF_{cat,0} \times t / p_{bet}}$. The dashed blue line corresponds to the third order term alone: $TON_{cat} = \sqrt[3]{3TOF_{cat,0} \times t / p_{bet} \frac{p_{betc}}{\gamma}}$ when $\frac{p_{betc}}{\gamma} = 10^{-2}$.

If $\frac{p_{betc}}{\gamma}$ is vanishing small, taking a reasonable value of

$p_{bet} = \frac{k_{bet}}{k_{ET}} = 3$, it is shown that the second order term is dominant (dashed red line in Figure 1). The kinetic information that can be retrieved is then $\frac{TOF_{cat,0}}{p_{bet}} = \frac{k_Q[\mathrm{SD}]}{k_b + k_Q[\mathrm{SD}]} \frac{[\mathrm{PS}]_0}{[\mathrm{Cat_{ox}}]_0} k_{abs} \frac{k_{ET}}{k_{bet}}$. Hence no information on the catalytic rate constant k is obtained in such a situation. Alternatively, if $\frac{p_{bet} p_{betc}}{\gamma p_{bet} + p_{betc}}$ is large enough, then the third term becomes quickly dominant (dashed blue line in Figure 1) and the kinetic information obtained from the plot is:

$$\frac{TOF_{cat,0}}{p_{bet}} \frac{\gamma}{p_{betc}} = \frac{k_Q[\mathrm{SD}]}{k_b + k_Q[\mathrm{SD}]} \frac{[\mathrm{PS}]_0}{([\mathrm{Cat_{ox}}]_0)^2} k_{abs} \frac{k_{ET}}{k_{bet}} \frac{k[\mathrm{S_{ox}}]_0}{k_{betc}}$$

It can provide information on the catalytic step provided all other rate constants are known independently. It is important to also emphasize that in all cases the retrieved information depends on k_{abs} which depends on experimental conditions determining how much light is ultimately absorbed by the photocatalytic solution. We also note that the shallow increase of TON_{cat} over time when the third order term is dominant may give the wrong impression that TON_{cat} plateaus. This might be the source of an incorrect interpretation.

Photoinduced catalysis: limiting processes

Photoinduced catalysis of redox reactions are limited by degradation of one or multiple components of the system. Examination of all possible degradation processes is not possible as they may be complex and they are often specific of a given system. We consider in the following the effect of two pathways on the maximal turnover number. These pathways are: (i) first order irreversible degradation of the reduced form of the catalyst (rate constant k_c (s^{-1}), Scheme 2), and (ii) first order irreversible degradation of the reduced photosensitizer (rate constant k_i (s^{-1}), Scheme 2). Following the methodology presented here, adaptation to other degradation processes corresponding to specific experimental systems is possible. In the presence of one of considered degradation pathways, TON_{cat} reaches a limiting value $TON_{cat}^{\lim}$ which expression is given in Table 1 (see SI for details on the derivation). Experimentally, analysis of the solution at the end of an experiment should allow knowing which component has been degraded, catalyst, photosensitizer, or both. We assume here that one degradation pathway is prevalent and that it determines $TON_{cat}^{\lim}$.

It is seen that in the case of degradation of the catalyst, the limiting value of $TON_{cat}^{\lim,c}$ is equal to the inverse of the competition parameter $p_c = \frac{k_c}{k[\mathrm{S_{ox}}]}$. Importantly, $TON_{cat}^{\lim,c}$ is independent on both the concentration of the catalyst and the concentration of the photosensitizer. It can thus be used as a criteria to identify or discard such a degradation pathway. It is also interesting to note that $TON_{cat}^{\lim,c}$ has the same expression as the maximal turnover number if the same reduction (S_{ox} to P_{red}) is driven electrochemically catalyzed by the same homogeneous catalyst (Cat_{ox}) undergoing a first order degradation in its reduced form. [40]

Scheme 2. Reductive quenching in photoinduced catalysis of redox reactions with degradation processes.

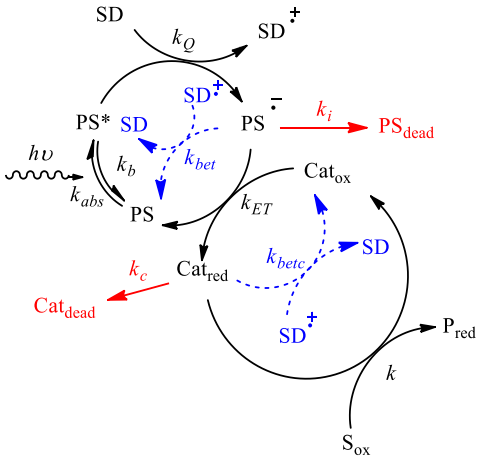

The time evolution of TON_{cat} in the presence of catalyst degradation depends on the three dimensionless parameters p_{bet}, $\frac{p_{betc}}{\gamma}$ and p_c as well as on $TOF_{cat,0}$ via an implicit expression (see SI for derivation):

$$\left(TON_{cat} + \frac{p_{betc}}{\gamma}(1+p_c)\frac{TON_{cat}^{\,2}}{2}\right) - \left[p_{bet}(1+p_c)\right]\left[\frac{TON_{cat}}{p_c} + \frac{1}{p_c^{\,2}}\ln(1-p_c TON_{cat})\right] - \frac{p_{bet}\frac{p_{betc}}{\gamma}(1+p_c)^2}{p_c^{\,3}}\left[\frac{3}{2} + \frac{(1-p_c TON_{cat})^2}{2} - 2(1-p_c TON_{cat}) + \ln(1-p_c TON_{cat})\right] = TOF_{cat,0} \times t \quad (5)$$

Table 1. Limiting value of the turnover number.

Limiting process	$TON_{cat}^{\lim}$ expression
Cat_{red} degradation	$TON_{cat}^{\lim,c} = \frac{1}{p_c}$ with $p_c = \frac{k_c}{k[\mathrm{S_{ox}}]}$
$PS^{\bullet-}$ degradation	$TON_{cat}^{\lim,i} = \frac{\gamma}{p_{betc}}\left(-1+\sqrt{1+2\frac{p_{betc}}{\gamma p_i}}\right)$ with $p_i = \frac{k_i}{k_{ET}[\mathrm{PS}]_0}$

Figure 2 exemplifies the effect of catalyst degradation on the time evolution of the turnover number according to equation (5).

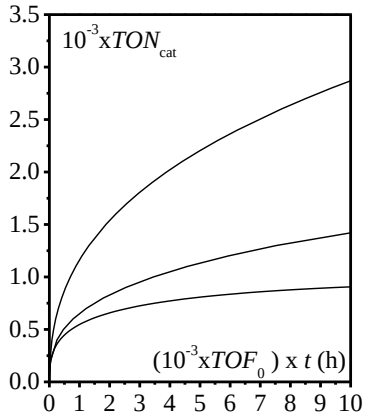

Figure 2. Time evolution of the turnover number in photoinduced catalysis of a redox reaction for a system with catalyst degradation for various values of $p_c = 0$, 10^{-4}, 10^{-3} (from top to bottom) with $p_{bet} = 3$ and $\frac{p_{betc}}{\gamma} = 10^{-3}$. Note that the limiting values are not reached.

We now consider the degradation of the reduced form of the photosensitizer via a first order reaction as the only degradation pathway. We obtain that the maximal turnover number depends on the value of $\frac{p_{betc}}{\gamma p_i} = \frac{k_{betc}\left[\mathrm{Cat_{ox}}\right]_0}{k\left[\mathrm{S_{ox}}\right]_0}\frac{k_{ET}\left[\mathrm{PS}\right]_0}{k_i}$ (Table 1, see SI for derivation details). If $\frac{p_{betc}}{\gamma p_i}$ is small compared to unity, then $TON_{cat}^{\lim,i} = \frac{k_{ET}\left[\mathrm{PS}\right]_0}{k_i}$, independent on the catalyst concentration but proportional to the photosensitizer concentration. If $\frac{p_{betc}}{\gamma p_i}$ is large compared to unity, then $TON_{cat}^{\lim,i} \approx \sqrt{2\frac{k\left[\mathrm{S_{ox}}\right]_0}{k_{betc}\left[\mathrm{Cat_{ox}}\right]_0}\frac{k_{ET}\left[\mathrm{PS}\right]_0}{k_i}}$ and therefore proportional to the square root of the concentration of the photosensitizer and inversely proportional to the square root of the catalyst concentration. Interestingly, an increase of $TON_{cat}^{\lim}$ was indeed reported in various studies upon lowering the catalyst concentration. [41,42,43] It was proposed that this phenomenon occurs because only a fraction of the catalyst molecules is active at high concentration while the remainder acts as a reservoir when the catalyst is progressively deactivated over time. [43] However, we show here that this phenomena can occur without deactivation of the catalyst. Variations of $TON_{cat}^{\lim,i}$ with the photosensitizer and the catalyst concentration can be used as criteria to analyze the degradation process in a photoinduced catalysis of a redox reaction. The time evolution of the turnover number is governed by a differential equation (see SI for derivation) depending on γ, p_{bet}, $\frac{p_{betc}}{\gamma}$, p_i as well as on $TOF_{cat,0}$:

$$\frac{dTON_{cat}}{dt} = \left(\frac{1}{1+\frac{p_{betc}}{\gamma}TON_{cat}} + p_i\gamma\right)\frac{TOF_{cat,0}}{\left(1+p_{bet}TON_{cat}\right)} \times\left\{1-\frac{TON_{cat}}{\gamma}+\frac{1}{p_{betc}}\frac{1}{p_i\gamma}\ln\left[1+\frac{TON_{cat}}{\frac{\gamma}{p_{betc}}\left(\frac{1}{p_i\gamma}+1\right)}\right]\right\} \quad (6)$$

Numerical resolution of this differential equation allows getting typical profiles of the time evolution of the turnover number for various values of p_i for a given set of γ, p_{bet}, $\frac{p_{betc}}{\gamma}$ values as exemplified in Figure 3.

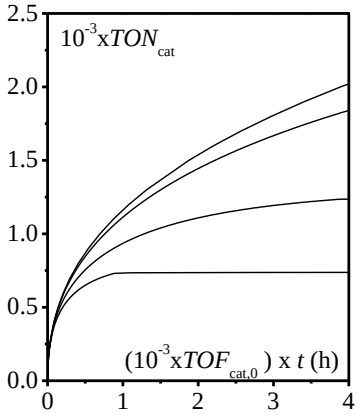

Figure 3. Time evolution of the turnover number in photoinduced catalysis of a redox reaction for a system with photosensitizer degradation for various values of $p_i = 0$, 10^{-4}, $5\ 10^{-4}$, 10^{-3} (from top to bottom) with $\gamma = 100$, $p_{bet} = 3$ and $\frac{p_{betc}}{\gamma} = 10^{-2}$.

Photoinduced catalysis: light-driven hydrogen production

The present kinetic analysis framework is now used as a framework to analyze previously reported experimental data of light-driven hydrogen production in water. Many experimental systems have been described in the literature in which photoinduced catalysis of hydrogen evolution is carried out in aqueous media at pH 4-5 with ascorbate (Scheme 3, HA^-) as sacrificial donor, a molecular photosensitizer, often $Ru(bpy)_3^{2+}$ (Scheme 3, Ru) and a molecular catalyst, often a cobalt complex.[18,41,44-64] In particular, some of us have reported that remarkable performances can be obtained by associating an hydrosoluble tris(ethoxyethanol)-triazatriangulenium photosensitizer (Scheme 3, $TATA^+$) and an efficient catalyst, a cobalt tetrazamacrocyclic complex $[Co^{III}(CR14)Cl_2]^+$ (Scheme 3, **1**).[65]

Scheme 3. Photosensitizers, sacrificial donor and catalyst considered in this work

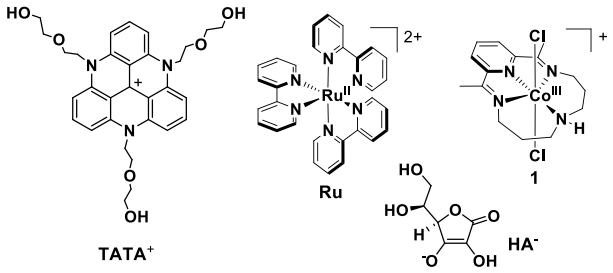

Quasi-ideal system: $TATA^+$ as photosensitizer

Application of the present kinetic model to the previously reported data requires an adaptation to take into account the stoichiometry of the redox reaction, which is equal to 2 for hydrogen production. Considering a reaction scheme in which an intermediate I (here a cobalt hydride) is first formed and then easily reduced by the catalyst to give the product (hydrogen) via reaction with a second proton donor molecule (Scheme 4), it is shown in the SI that, provided the intermediate I is at steady-state, the time evolution of the turnover number of an ideal system is given by (instead of equation (4)):

$$TON_{cat} + \left(\frac{p_{betc,2}}{\gamma} + \frac{p_{bet}}{2}\right)\left(TON_{cat}\right)^2 + \frac{4}{3}\,p_{bet}\,\frac{p_{betc,2}}{\gamma}\left(TON_{cat}\right)^3 = TOF_{cat,0,2} \times t \qquad (7)$$

with $TOF_{cat,0,2} = \gamma\, p_Q k_{abs} / 2$, $\frac{p_{betc,2}}{\gamma} = \frac{k_{betc}\left[\mathrm{Cat}_{ox}\right]_0}{2k_1\left[\mathrm{S}_{ox}\right]_0}$.

$k_1\left[\mathrm{S}_{ox}\right]_0$ can also be noted k_{cat}, a pseudo first order catalytic rate. All other parameters have the same definition as in the one electron scheme. We note that the intermediate I can be alternatively reduced by Cat_{red}. However, $PS^{\bullet-}$ is a stronger reductant than Cat_{red}. Moreover, as shown in the SI, both $PS^{\bullet-}$ and Cat_{red} are at steady-state and their concentrations are related as follows: $\left[\mathrm{Cat}_{red}\right] = \left[\mathrm{PS}^{\bullet-}\right]\frac{k_{ET}\left[\mathrm{Cat}_{ox}\right]}{k_1\left[\mathrm{S}_{ox}\right] + k_{betc}\left[\mathrm{SD}^{\bullet+}\right]}$. Taking into account that $k_1\left[\mathrm{S}_{ox}\right] + k_{betc}\left[\mathrm{SD}^{\bullet+}\right]$ is the inverse of the lifetime of Cat_{red} which has been estimated to be ca. 140 µs, [65] and $k_{ET}\left[\mathrm{Cat}_{ox}\right] \approx 5\ 10^3\ s^{-1}$, we have $\left[\mathrm{Cat}_{red}\right]/\left[\mathrm{PS}^{\bullet-}\right] \approx 0.7$, we only consider the reduction of I by $PS^{\bullet-}$.

Scheme 4. Reductive quenching in photoinduced catalysis of two electrons redox reactions.

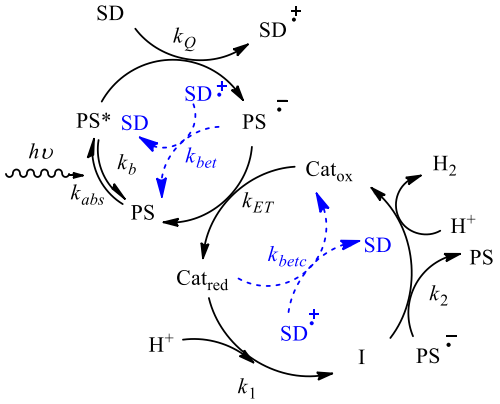

Previous photophysical and transient absorption measurements have led to the determination of several rate constants for the present experimental system, namely k_b, k_Q, k_{bet}, k_{betc} and k_{ET}. [65] These data are gathered in Table 2 and their determination recalled in the SI.

Table 2. Rate constants of experimental systems

Photosensitizer	$TATA^+$	$Ru(bpy)_3^{2+}$
k_b (s^{-1})	$7.14\ 10^7$	$1.65\ 10^6$
k_Q ($M^{-1}s^{-1}$)	$3.6\ 10^9$	$2.5\ 10^7$
k_{bet} ($M^{-1}s^{-1}$)	$3.26\ 10^9$	$3.5\ 10^9$
k_{betc} ($M^{-1}s^{-1}$)	$2.6\ 10^7$	$2.6\ 10^7$
k_{ET} ($M^{-1}s^{-1}$)	$7.35\ 10^8$	$1.4\ 10^9$
$k_{cat} = k_1\left[\mathrm{S}_{ox}\right]_0$ (s^{-1})	$7.1\ 10^3$	$7.1\ 10^3$
k_{abs} (s^{-1})	$3.16\ 10^3$	$1.3\ 10^3$

These rate constants are used to fit the experimental data recorded with $[TATA^+]$ = 500 µM and [**1**]= 2.5, 5 and 10 µM, hence $\gamma = 200$, 100, 50 respectively. Taking into account that the concentration of the sacrificial donor was $[HA^-]$ = 0.076 M, $p_Q = \frac{k_Q\left[\mathrm{HA}^-\right]}{k_b + k_Q\left[\mathrm{HA}^-\right]} = 0.79$. Rate constants given in Table 2 provide $p_{bet} = \frac{k_{bet}}{k_{ET}} = 4.435$, $p_{betc} = \frac{k_{betc}\left[\mathrm{TATA}^+\right]_0}{2k_{cat}} = 0.915$. Data are fitted with equation (7) thus considering the system as ideal since only little degradation of the photosensitizer was observed experimentally.[65] Figure 4 shows the fitting of the kinetic expression (7) to the experimental data via adjustment of a simple parameter k_{abs} = $3.16\ 10^3\ s^{-1}$. This rate constant characterizing light absorption by the photosensitizer $TATA^+$ is obviously dependent on the irradiation conditions. To check that our analysis with an analytical model is valid, we have performed additional simulations using a Kinetics Simulator Gepasi (see SI and Figure S1).

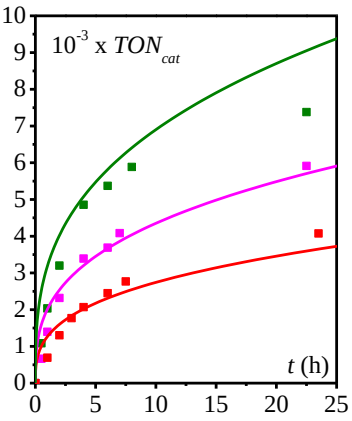

Figure 4. Photocatalytic hydrogen production (TON_{cat}) as a function of time from a deaerated 1 M acetate buffer (5 mL) at pH 4.5 under visible-light irradiation in the presence of $TATA^+$ (0.5 mM), $NaHA/H_2A$ (0.1 M) and various concentration of the catalyst $[Co^{III}(CR14)Cl_2]^+$: 2.5 µM (green), 5 µM (magenta) and 10 µM (red). Square: experimental data (from reference [65]). Lines: simulations (see text).

The analysis shows that our kinetic model is capturing the essential features of the system. In turn, it shows that photophysical and transient absorption measurements can be used to predict the behavior of the system provided the system is stable (ideal) and light absorption properties are known. As another outcome, this analysis illustrates that the time evolution of the turnover number is a complex combination of several phenomena, i.e. light absorption, quenching, electron transfer, catalysis that cannot be easily disentangle. Hence, the simple report of the apparent initial turnover frequency and the turnover number on a large irradiation time are not a reliable metrics to compare systems.

Photosensitizer degradation: $Ru(bpy)_3^{2+}$ as photosensitizer

$Ru(bpy)_3^{2+}$ is a commonly used photosensitizer due to its long lived excited state and good reducing properties of the reduced state $[Ru(bpy)2(bpy^{\bullet-})]^+$. However, comparison of the light driven hydrogen production with both $TATA^+$ and $Ru(bpy)_3^{2+}$ as photosensitizer in identical conditions shows significant differences. Whereas the behavior of the system can be considered as quasi-ideal over 24 hours of irradiation with $TATA^+$ as photosensitizer (vide supra), TON_{cat} quickly levels off when $Ru(bpy)_3^{2+}$ is used as photosensitizer (Figure 5).[65] This is attributed to the well-known degradation of the reduced form $[Ru(bpy)_2(bpy^{\bullet-})]^+$ which undergoes substitution of one of its bipyridine ligand in acidic aqueous solution by solvent molecules and/or anions such as ascorbate.[41,59] We therefore analyze the previously reported data in the framework of a mechanism depicted in Scheme 5: a two electrons photoinduced catalytic process is considered with an intermediate I (here a cobalt hydride) at steady-state. First order degradation of the reduced form of the photosensitizer is considered as the only deactivation pathway.

Scheme 5. Reductive quenching in photoinduced catalysis of two electrons redox reactions with photosensitizer degradation.

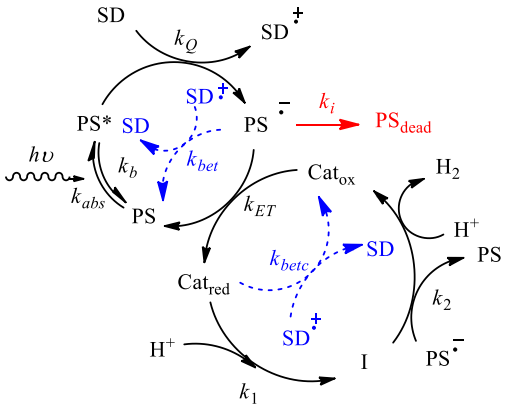

Because of the two electrons stoichiometry, the kinetic model presented in the previous sections has to be adapted (see SI), leading to replacement of the governing differential equation (6) by equation (8):

$$\frac{dTON_{cat}}{dt} = \frac{2TOF_{cat,0,2}\left[1 - p_i\left(TON_{cat} + 2\frac{p_{betc,2}}{\gamma}TON_{cat}^{\,2}\right)\right]}{\left(1 + 2p_{bet}TON_{cat} + p_i\gamma\right)\left(1 + 4\frac{p_{betc,2}}{\gamma}TON_{cat}\right) + 1} \qquad (8)$$

with, $TOF_{cat,0,2} = \gamma p_Q k_{abs}/2$, $\frac{p_{betc,2}}{\gamma} = \frac{k_{betc}\left[\mathrm{Cat_{ox}}\right]_0}{2k_1\left[\mathrm{S_{ox}}\right]_0}$. All other parameters have the same definition as in the one electron scheme. As in the case of $TATA^+$, rate constants are known from previous photophysical and transient absorption measurements (k_b , k_Q , k_{bet} , k_{betc} , k_{ET} , k_{cat}) and gathered in Table 2 (see SI for details). These rate constants are used to fit the experimental data recorded with $[Ru(bpy)_3^{2+}]$ = 500 µM and [**1**]= 5 and 10 µM, hence γ = 100, 50 respectively. Taking into account that the concentration of the sacrificial donor was $[HA^-]$ = 0.076 M, $p_Q = \frac{k_Q\left[\mathrm{HA^-}\right]}{k_b + k_Q\left[\mathrm{HA^-}\right]}$ = 0.535. Rate constants given in Table 2 provide $p_{bet} = \frac{k_{bet}}{k_{ET}} = 2.5$, $p_{betc} = \frac{k_{betc}\left[\mathrm{Ru(bpy)_3^{2+}}\right]_0}{2k_{cat}} = 0.915$. Assuming that $p_i = \frac{k_i}{k_{ET}\left[\mathrm{Ru(bpy)_3^{2+}}\right]_0}$ is small compared to unity, it is shown (see SI), that the limited turnover number is:

$$TON_{cat}^{\lim,i} = \frac{\gamma}{4p_{betc}}\left(-1 + \sqrt{1 + 8\frac{p_{betc}}{\gamma p_i}}\right) \qquad (9)$$

Therefore, application of equation (9) to the experimental data (Figure 5) leads to p_i = 1.88 10^{-5} and 1.28 10^{-5} (i.e. much smaller than 1, thus validating the assumption) for γ = 50

and 100 respectively, hence corresponding to $k_i = 13.2\ s^{-1}$ and 9 s^{-1} respectively. Both values are close indicating that considering a first order degradation of $[Ru(bpy)_2(bpy^{\bullet-})]^+$ as limiting process is reasonable. The time evolution of TON_{cat} was then simulated by numerical resolution of equation (8) and adjustment of $TOF_{cat,0,2} = \gamma p_Q k_{abs} / 2$. We obtain $k_{abs} = 1.3\ 10^3\ s^{-1}$.

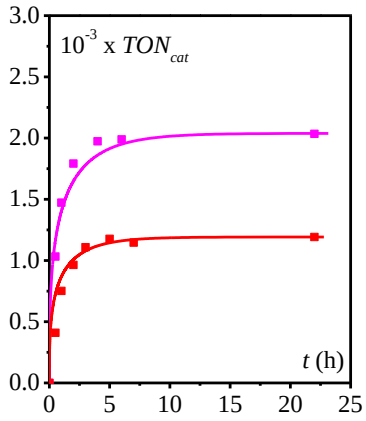

Figure 5. Photocatalytic hydrogen production (TON_{cat}) as a function of time from a deaerated 1 M acetate buffer (5 mL) at pH 4.5 under visible-light irradiation in the presence of $Ru(bpy)_3^{2+}$ (0.5 mM), NaHA/H_2A (0.1 M) and various concentration of the catalyst $[Co^{III}(CR14)Cl_2]^+$: 5 µM (magenta) and 10 µM (red). Square: experimental data (from reference [65]). Lines: simulations (see text).

The parameters controlling the evolution of the turnover number as function of time with both $TATA^+$ and $Ru(bpy)_3^{2+}$ are summarized in Table 3.

Table 3. Parameters

Photosensitizer	$TATA^+$	$Ru(bpy)_3^{2+}$
p_Q	0.79	0.535
p_{bet}	4.435	2.5
p_{betc}	0.915	0.915
p_i	0	ca. $1.5\ 10^{-5}$
$\frac{TOF_{cat,0,2}}{\gamma}$ (s^{-1})	2496	695

The superiority of $TATA^+$ over $Ru(bpy)_3^{2+}$ as a photosensitizer is due not only to the higher stability of its reduced form (p_i smaller) but also to the faster formation of this reduced form (higher $\frac{TOF_{cat,0,2}}{\gamma} = p_Q k_{abs}$) due to a slightly higher ability to absorb the light from the irradiation lamp (higher k_{abs}) combined with a more efficient quenching of the excited state by the sacrificial donor (higher p_Q). This is however balanced by a larger contribution of the back electron transfer (higher p_{bet}) in the case of $TATA^+$ vs. $Ru(bpy)_3^{2+}$ making more photoinduced generation of the reduced form of the photosensitizer unproductive.

Conclusion

The bases have been laid for a kinetic analysis of photoinduced catalytic systems. The proposed kinetic model provides an analytical expression of the turnover number vs. time as function of dimensionless parameters related to the rate constant of the key-steps of the system. As an important result, we show that, even for an ideal system where no degradation occurs and with excess of substrates, the turnover number does not increase linearly with time due to of both increasing contribution of back electron transfers. Taking into account the possibilities of degradation of either the reduced photosensitizer or the reduced form of the catalyst, it is remarkable that, in each case, an analytical expression of the limiting turnover number is obtained which depends on well-identified dimensionless parameters. These expressions provide a useful tool in the aim to optimize a given system. For example, in the case of a limitation is due to the photosensitizer degradation, the maximal turnover number not only depends on the ratio of the rate constants of electron transfer to the catalyst from the reduced form of the photosensitizer and its deactivation rate constant (p_i) but it also depends on a parameter characterizing the back electron transfer from the reduced catalyst (p_{betc} / γ).

The kinetic model presented for a simple one electron redox reaction considering a reductive quenching catalytic process can be easily adapted to other situations, namely oxidative quenching and multiple electron transfer reactions. We have indeed extended the kinetic model to a two electrons transfer process adequate for an analysis of light-induced hydrogen production in water. The model has been successfully applied to recently reported experimental data. It is seen that using an hydrosoluble tris(ethoxyethanol)-triazatriangulenium photosensitizer in association with a cobalt tetrazamacrocyclic complex as catalyst together with ascorbate as sacrificial donor, the system behaves as a quasi-ideal system. Alternatively, using the classical $Ru(bpy)_3^{2+}$ as a photosensitizer, the turnover number quickly levels off due to the degradation of the reduced form $[Ru(bpy)_2(bpy^{\bullet-})]^+$. Interestingly, our thorough analysis allows deciphering the intrinsic reasons underlying the observation that the rising part of the turnover vs. time is similar with the use of either photosensitizer. We hope that our approach will stimulate kinetic analysis of various systems in the near future to the benefit of a lucid benchmarking of photoinduced catalytic systems.

ASSOCIATED CONTENT

Supporting Information

Derivation of equations. Numerical simulations. Details on experimental data.

AUTHOR INFORMATION

Corresponding Author

cyrille.costentin@univ-grenoble-alpes.fr

Notes

The author declares no competing financial interest.

ACKNOWLEDGMENT

This work was partially supported by the Agence Nationale de la Recherche (Labex ARCANE, CBH-EUR-GS, ANR-17-EURE-0003).

REFERENCES

(1) Berardi, S.; Drouet, S.; Francas, L.; Gimbert-Surinach, C.; Guttentag, M.; Richmond, C.; Stoll, T.; Llobet, A.: Molecular Artificial Photosynthesis. *Chemical Society Reviews* **2014**, *43*, 7501-7519.

(2) Zhang, B.; Sun, L.: Artificial photosynthesis: opportunities and challenges of molecular catalysts. *Chemical Society Reviews* **2019**, *48*, 2216-2264.

(3) Artero, V.; Chavarot-Kerlidou, M.; Fontecave, M.: Splitting Water with Cobalt. *Angew. Chem. Int. Ed.* **2011**, *50*, 7238-7266.

(4) Li, X.-B.; Tung, C.-H.; Wu, L.-Z.: Semiconducting quantum dots for artificial photosynthesis. *Nature Reviews Chemistry* **2018**, *2*, 160-173.

(5) Stolarczyk, J. K.; Bhattacharyya, S.; Polavarapu, L.; Feldmann, J.: Challenges and Prospects in Solar Water Splitting and CO2 Reduction with Inorganic and Hybrid Nanostructures. *ACS Catalysis* **2018**, *8*, 3602-3635.

(6) Wen, F.; Li, C.: Hybrid Artificial Photosynthetic Systems Comprising Semiconductors as Light Harvesters and Biomimetic Complexes as Molecular Cocatalysts. *Accounts of Chemical Research* **2013**, *46*, 2355-2364.

(7) Dalle, K. E.; Warnan, J.; Leung, J. J.; Reuillard, B.; Karmel, I. S.; Reisner, E.: Electro- and Solar-Driven Fuel Synthesis with First Row Transition Metal Complexes. *Chemical Reviews* **2019**, *119*, 2752-2875.

(8) Young, K. J.; Martini, L. A.; Milot, R. L.; Snoeberger, R. C.; Batista, V. S.; Schmuttenmaer, C. A.; Crabtree, R. H.; Brudvig, G. W.: Light-driven water oxidation for solar fuels. *Coordination Chemistry Reviews* **2012**, *256*, 2503-2520.

(9) Sartorel, A.; Bonchio, M.; Campagna, S.; Scandola, F.: Tetrametallic molecular catalysts for photochemical water oxidation. *Chemical Society Reviews* **2013**, *42*, 2262-2280.

(10) Fukuzumi, S.; Jung, J.; Yamada, Y.; Kojima, T.; Nam, W.: Homogeneous and Heterogeneous Photocatalytic Water Oxidation by Persulfate. *Chemistry – An Asian Journal* **2016**, *11*, 1138-1150.

(11) Limburg, B.; Bouwman, E.; Bonnet, S.: Rate and Stability of Photocatalytic Water Oxidation using [Ru(bpy)3]2+ as Photosensitizer. *ACS Catalysis* **2016**, *6*, 5273-5284.

(12) Duan, L. L.; Tong, L. P.; Xu, Y. H.; Sun, L. C.: Visible light-driven water oxidation-from molecular catalysts to photoelectrochemical cells. *Energy & Environmental Science* **2011**, *4*, 3296-3313.

(13) Parent, A. R.; Sakai, K.: Progress in Base-Metal Water Oxidation Catalysis. *Chemsuschem* **2014**, *7*, 2070-2080.

(14)Collomb, M.-N.; Morales, D. V.; Astudillo, C. N.; Dautreppe, B.; Fortage, J.: Hybrid photoanodes for water oxidation combining a molecular photosensitizer with a metal oxide oxygen-evolving catalyst. *Sustainable Energy & Fuels* **2020**, *4*, 31-49.

(15) Sutin, N.; Creutz, C.; Fujita, E.: Photo-induced generation of dihydrogen and reduction of carbon dioxide using transition metal complexes. *Comments on Inorganic Chemistry* **1997**, *19*, 67-92.

(16) Eckenhoff, W. T.; Eisenberg, R.: Molecular systems for light driven hydrogen production. *Dalton Transactions* **2012**, *41*, 13004-13021.

(17) Stoll, T.; Castillo, C. E.; Kayanuma, M.; Sandroni, M.; Daniel, C.; Odobel, F.; Fortage, J.; Collomb, M.-N.: Photo-Induced Redox Catalysis for Proton Reduction to Hydrogen with Homogeneous Molecular Systems using Rhodium-Based Catalysts. *Coordination Chemistry Reviews* **2015**, *304–305*, 20-37.

(18) Queyriaux, N.; Jane, R. T.; Massin, J.; Artero, V.; Chavarot-Kerlidou, M.: Recent developments in hydrogen evolving molecular cobalt(II)–polypyridyl catalysts. *Coordination Chemistry Reviews* **2015**, *304*, 3-19.

(19) Fukuzumi, S.; Lee, Y.-M.; Nam, W.: Thermal and photocatalytic production of hydrogen with earth-abundant metal complexes. *Coordination Chemistry Reviews* **2018**, *355*, 54-73.

(20) Eckenhoff, W. T.: Molecular catalysts of Co, Ni, Fe, and Mo for hydrogen generation in artificial photosynthetic systems. *Coordination Chemistry Reviews* **2018**, *373*, 295-316.

(21) Dempsey, J. L.; Brunschwig, B. S.; Winkler, J. R.; Gray, H. B.: Hydrogen Evolution Catalyzed by Cobaloximes. *Accounts of Chemical Research* **2009**, *42*, 1995-2004.

(22) Willkomm, J.; Orchard, K. L.; Reynal, A.; Pastor, E.; Durrant, J. R.; Reisner, E.: Dye-Sensitized Semiconductors Modified with Molecular Catalysts for Light-Driven H_2 Production. *Chem. Soc. Rev.* **2016**, *45*, 9-23.

(23) Hutton, G. A. M.; Martindale, B. C. M.; Reisner, E.: Carbon dots as photosensitisers for solar-driven catalysis. *Chemical Society Reviews* **2017**, *46*, 6111-6123.

(24) Sandroni, M.; Gueret, R.; Wegner, K. D.; Reiss, P.; Fortage, J.; Aldakov, D.; Collomb, M. N.: Cadmium-free $CuInS_2$/ZnS quantum dots as efficient and robust photosensitizers in combination with a molecular catalyst for visible light-driven H_2 production in water. *Energy & Environmental Science* **2018**, *11*, 1752-1761.

(25) Call, A.; Franco, F.; Kandoth, N.; Fernandez, S.; Gonzalez-Bejar, M.; Perez-Prieto, J.; Luis, J. M.; Lloret-Fillol, J.: Understanding light-driven H2 evolution through the electronic tuning of aminopyridine cobalt complexes. *Chemical Science* **2018**, *9*, 2609-2619.

(26) Corredor, J.; Rivero, M. J.; Rangel, C. M.; Gloaguen, F.; Ortiz, I.: Comprehensive review and future perspectives on the photocatalytic hydrogen production. *Journal of Chemical Technology & Biotechnology* **2019**, *94*, 3049-3063.

(27) Gao, S.; Fan, W.; Liu, Y.; Jiang, D.; Duan, Q.: Artificial water-soluble systems inspired by [FeFe]-hydrogenases for electro- and photocatalytic hydrogen production. *International Journal of Hydrogen Energy* **2020**, *45*, 4305-4327.

(28) Mazzeo, A.; Santalla, S.; Gaviglio, C.; Doctorovich, F.; Pellegrino, J.: Recent progress in homogeneous light-driven hydrogen evolution using first-row transition metal

catalysts. *Inorganica Chimica Acta* **2020**, *517*, 119950.

(29) Yamazaki, Y.; Takeda, H.; Ishitani, O.: Photocatalytic reduction of CO_2 using metal complexes. *Journal of Photochemistry and Photobiology C: Photochemistry Reviews* **2015**, *25*, 106-137.

(30) Boutin, E.; Merakeb, L.; Ma, B.; Boudy, B.; Wang, M.; Bonin, J.; Anxolabéhère-Mallart, E.; Robert, M.: Molecular catalysis of CO_2 reduction: recent advances and perspectives in electrochemical and light-driven processes with selected Fe, Ni and Co aza macrocyclic and polypyridine complexes. *Chemical Society Reviews* **2020**, *49*, 5772-5809.

(31) Perazio, A.; Lowe, G.; Gobetto, R.; Bonin, J.; Robert, M.: Light-driven catalytic conversion of CO_2 with heterogenized molecular catalysts based on fourth period transition metals. *Coordination Chemistry Reviews* **2021**, *443*, 214018.

(32) Chen, L.; Chen, G.; Leung, C.-F.; Cometto, C.; Robert, M.; Lau, T.-C.: Molecular quaterpyridine-based metal complexes for small molecule activation: water splitting and CO_2 reduction. *Chemical Society Reviews* **2020**, *49*, 7271-7283.

(33) Li, D.; Kassymova, M.; Cai, X.; Zang, S.-Q.; Jiang, H.-L.: Photocatalytic CO_2 reduction over metal-organic framework-based materials. *Coordination Chemistry Reviews* **2020**, *412*, 213262.

(34) Yuan, Y.-J.; Yu, Z.-T.; Chen, D.-Q.; Zou, Z.-G.: Metal-Complex Chromophores for Solar Hydrogen Generation. *Chemical Society Reviews* **2017**, *46*, 603-631.

(35) Rao, H.; Lim, C. H.; Bonin, J.; Miyake, G. M.; Robert, M.: Visible-Light-Driven Conversion of CO_2 to CH_4 with an Organic Sensitizer and an Iron Porphyrin Catalyst. *Journal of the American Chemical Society* **2018**, *140*, 17830-17834.

(36) Rao, H.; Schmidt, L. C. S.; Bonin, J.; Robert, M.: Visible-light-driven methane formation from CO_2 with a molecular iron catalyst. *Nature* **2017**, *548*, 74-+.

(37) Queyriaux, N.; Giannoudis, E.; Windle, C. D.; Roy, S.; Pecaut, J.; Coutsolelos, A. G.; Artero, V.; Chavarot-Kerlidou, M.: A noble metal-free photocatalytic system based on a novel cobalt tetrapyridyl catalyst for hydrogen production in fully aqueous medium. *Sustainable Energy & Fuels* **2018**, *2*, 553-557.

(38) Pellegrin, Y.; Odobel, F.: Sacrificial Electron Donor Reagents for Solar Fuel Production. *C. R. Chim.* **2017**, *20*, 283-295.

(39) To decrease back electron transfer, irreversible sacrifical donors are used. However, in many cases, species resulting from the chemical evolution of the oxidized sacrifical donor may also be involved in a back electron transfer reaction.

(40) Costentin, C.; Passard, G.; Savéant, J.-M.: Benchmarking of Homogeneous Electrocatalysts: Overpotential, Turnover Frequency, Limiting Turnover Number. *Journal of the American Chemical Society* **2015**, *137*, 5461-5467.

(41) Khnayzer, R. S.; Thoi, V. S.; Nippe, M.; King, A. E.; Jurss, J. W.; El Roz, K. A.; Long, J. R.; Chang, C. J.; Castellano, F. N.: Towards a Comprehensive Understanding of Visible-Light Photogeneration of Hydrogen from Water Using Cobalt(II) Polypyridyl Catalysts. *Energy & Environmental Science* **2014**, *7*, 1477-1488.

(42) Thoi, V. S.; Kornienko, N.; Margarit, C. G.; Yang, P.; Chang, C. J.: Visible-Light Photoredox Catalysis: Selective Reduction of Carbon Dioxide to Carbon Monoxide by a Nickel N-Heterocyclic Carbene–Isoquinoline Complex. *Journal of the American Chemical Society* **2013**, *135*, 14413-14424.

(43) Guo, Z.; Cheng, S.; Cometto, C.; Anxolabéhère-Mallart, E.; Ng, S.-M.; Ko, C.-C.; Liu, G.; Chen, L.; Robert, M.; Lau, T.-C.: Highly Efficient and Selective Photocatalytic CO_2 Reduction by Iron and Cobalt Quaterpyridine Complexes. *Journal of the American Chemical Society* **2016**, *138*, 9413-9416.

(44) Stoll, T.; Gennari, M.; Serrano, I.; Fortage, J.; Chauvin, J.; Odobel, F.; Rebarz, M.; Poizat, O.; Sliwa, M.; Deronzier, A.; Collomb, M.-N.: $[Rh^{III}(dmbpy)_2Cl_2]^+$ as a Highly Efficient Catalyst for Visible-Light-Driven Hydrogen Production in Pure Water: Comparison with Other Rhodium Catalysts. *Chemistry – A European Journal* **2013**, *19*, 782-792.

(45) Jurss, J. W.; Khnayzer, R. S.; Panetier, J. A.; El Roz, K. A.; Nichols, E. M.; Head-Gordon, M.; Long, J. R.; Castellano, F. N.; Chang, C. J.: Bioinspired design of redox-active ligands for multielectron catalysis: effects of positioning pyrazine reservoirs on cobalt for electro- and photocatalytic generation of hydrogen from water. *Chem. Sci.* **2015**, *6*, 4954-4972.

(46) Han, Z.; Eisenberg, R.: Fuel from Water: The Photochemical Generation of Hydrogen from Water. *Accounts of Chemical Research* **2014**, *47*, 2537-2544.

(47) Zhao, X.; Wang, P.; Long, M.: Electro- and Photocatalytic Hydrogen Production by Molecular Cobalt Complexes with Pentadentate Ligands. *Comments on Inorganic Chemistry* **2016**, 1-33.

(48) Leung, C. F.; Cheng, S. C.; Yang, Y.; Xiang, J.; Yiu, S. M.; Ko, C. C.; Lau, T. C.: Efficient photocatalytic water reduction by a cobalt(II) tripodal iminopyridine complex. *Catalysis Science & Technology* **2018**, *8*, 307-313.

(49) Lo, W. K. C.; Castillo, C. E.; Gueret, R.; Fortage, J.; Rebarz, M.; Sliwa, M.; Thomas, F.; McAdam, C. J.; Jameson, G. B.; McMorran, D. A.; Crowley, J. D.; Collomb, M.-N.; Blackman, A. G.: Synthesis, Characterization, and Photocatalytic H_2-Evolving Activity of a Family of $[Co(N_4Py)(X)]^{n+}$ Complexes in Aqueous Solution. *Inorganic Chemistry* **2016**, *55*, 4564-4581.

(50) Varma, S.; Castillo, C. E.; Stoll, T.; Fortage, J.; Blackman, A. G.; Molton, F.; Deronzier, A.; Collomb, M.-N.: Efficient Photocatalytic Hydrogen Production in Water Using a Cobalt(III) Tetraaza-Macrocyclic Catalyst: Electrochemical Generation of the Low-Valent Co(I) Species and its Reactivity Toward Proton Reduction. *Physical Chemistry Chemical Physics* **2013**, *15*, 17544-17552.

(51) Gueret, R.; Castillo, C. E.; Rebarz, M.; Thomas, F.;

Hargrove, A.-A.; Pécaut, J.; Sliwa, M.; Fortage, J.; Collomb, M.-N.: Cobalt(III) Tetraaza-Macrocyclic Complexes as Efficient Catalyst for Photoinduced Hydrogen Production in Water: Theoretical Investigation of the Electronic Structure of the Reduced Species and Mechanistic Insight. *Journal of Photochemistry and Photobiology B: Biology* **2015**, *152*, 82-94.

(52) Gueret, R.; Castillo, C. E.; Rebarz, M.; Thomas, F.; Sliwa, M.; Chauvin, J.; Dautreppe, B.; Pécaut, J.; Fortage, J.; Collomb, M.-N.: Cobalt(II) Pentaaza-Macrocyclic Schiff Base Complex as Catalyst for Light-Driven Hydrogen Evolution in Water: Electrochemical Generation and Theoretical Investigation of the One-Electron Reduced Species. *Inorganic Chemistry* **2019**, *58*, 9043-9056.

(53) Eckenhoff, W. T.; McNamara, W. R.; Du, P.; Eisenberg, R.: Cobalt Complexes as Artificial Hydrogenases for the Reductive Side of Water Splitting. *Biochim. Biophys. Acta., Bioenerg.* **2013**, *1827*, 958-973.

(54) Schnidrig, S.; Bachmann, C.; Müller, P.; Weder, N.; Spingler, B.; Joliat-Wick, E.; Mosberger, M.; Windisch, J.; Alberto, R.; Probst, B.: Structure–Activity and Stability Relationships for Cobalt Polypyridyl-Based Hydrogen-Evolving Catalysts in Water. *ChemSusChem* **2017**, *10*, 4570-4580.

(55) Call, A.; Codola, Z.; Acuna-Pares, F.; Lloret-Fillol, J.: Photo- and Electrocatalytic H2 Production by New First-Row Transition-Metal Complexes Based on an Aminopyridine Pentadentate Ligand. *Chem. - Eur. J.* **2014**, *20*, 6171-6183.

(56) Natali, M.: Elucidating the Key Role of pH on Light-Driven Hydrogen Evolution by a Molecular Cobalt Catalyst. *ACS Catalysis* **2017**, 1330-1339.

(57) Natali, M.; Badetti, E.; Deponti, E.; Gamberoni, M.; Scaramuzzo, F. A.; Sartorel, A.; Zonta, C.: Photoinduced hydrogen evolution with new tetradentate cobalt(ii) complexes based on the TPMA ligand. *Dalton Transactions* **2016**, *45*, 14764-14773.

(58) Tong, L. P.; Zong, R. F.; Thummel, R. P.: Visible Light-Driven Hydrogen Evolution from Water Catalyzed by A Molecular Cobalt Complex. *Journal of the American Chemical Society* **2014**, *136*, 4881-4884.

(59) Singh, W. M.; Baine, T.; Kudo, S.; Tian, S.; Ma, X. A. N.; Zhou, H.; DeYonker, N. J.; Pham, T. C.; Bollinger, J. C.; Baker, D. L.; Yan, B.; Webster, C. E.; Zhao, X.: Electrocatalytic and Photocatalytic Hydrogen Production in Aqueous Solution by a Molecular Cobalt Complex. *Angew. Chem. Int. Ed.* **2012**, *51*, 5941-5944.

(60) Shan, B.; Baine, T.; Ma, X. A. N.; Zhao, X.; Schmehl, R. H.: Mechanistic Details for Cobalt Catalyzed Photochemical Hydrogen Production in Aqueous Solution: Efficiencies of the Photochemical and Non-Photochemical Steps. *Inorganic Chemistry* **2013**, *52*, 4853-4859.

(61) Zhao, X.; Wang, P.; Long, M.: Electro- and Photocatalytic Hydrogen Production by Molecular Cobalt Complexes With Pentadentate Ligands. *Comments on Inorganic Chemistry* **2017**, *37*, 238-270.

(62) Hogue, R. W.; Schott, O.; Hanan, G. S.; Brooker, S.: A Smorgasbord of 17 Cobalt Complexes Active for Photocatalytic Hydrogen Evolution. *Chemistry – A European Journal* **2018**, *24*, 9820-9832.

(63) Kohler, L.; Niklas, J.; Johnson, R. C.; Zeller, M.; Poluektov, O. G.; Mulfort, K. L.: Molecular Cobalt Catalysts for H2 Generation with Redox Activity and Proton Relays in the Second Coordination Sphere. *Inorganic Chemistry* **2018**, *58*, 1697-1709.

(64) Joliat-Wick, E.; Weder, N.; Klose, D.; Bachmann, C.; Spingler, B.; Probst, B.; Alberto, R.: Light-Induced H2 Evolution with a Macrocyclic Cobalt Diketo-Pyrphyrin as a Proton-Reducing Catalyst. *Inorganic Chemistry* **2018**, *57*, 1651-1655.

(65) Gueret, R.; Poulard, L.; Oshinowo, M.; Chauvin, J.; Dahmane, M.; Dupeyre, G.; Lainé, P. P.; Fortage, J.; Collomb, M.-N.: Challenging the $[Ru(bpy)_3]^{2+}$ Photosensitizer with a Triazatriangulenium Robust Organic Dye for Visible-Light-Driven Hydrogen Production in Water. *ACS Catalysis* **2018**, *8*, 3792-3802.

TOC

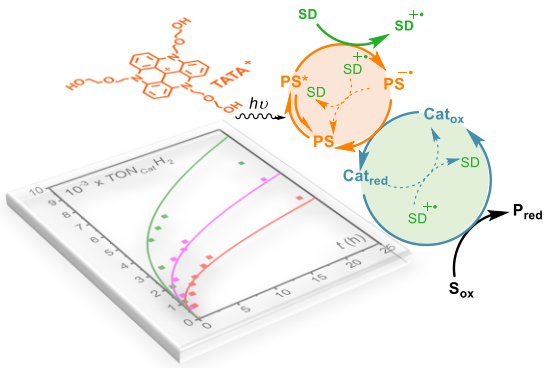
TATA+
hυ
SD
SD+•
PS*
SD
PS−•
PS
Catox
Catred
SD
SD+•
Pred
Sox
10³ x TON Cat H2
t (h)